Journal of Beijing Institute of Technology, 2021, Vol. 30, No. 4

Waveform Design for MIMO Radar with One-Bit DACs via Block-Sparse Semidefinite Relaxation

Tong Wei, Bin Liao✉

Abstract: Multiple-input multiple-output (MIMO) systems which deploy one-bit DACs are attractive in many fields, such as wireless communications and radar. In this paper, the problem of transmit waveform design in MIMO radar system with one-bit DACs is investigated. By appropriately designing the transmitted QPSK signal waveforms, the majority of radiated energy can be focused into the mainlobe region(s) by minimizing the integrated sidelobe to mainlobe ratio (ISMR) of beampattern, such that the intensity of backscattered signals from targets can be enhanced. However, the resulting optimization problem which consists of constrained fractional quadratic problem (CFQP) is noconvex. To tackle this problem, a block-sparse semidefinite relaxation method is first utilized to reformulate the CFQP into a reduced convex semidefinite programming (SDP). Further, a customized interior point algorithm (IPA) is developed to solve the small-scale SDP. Finally, the desirable one-bit transmit waveform sequence can be properly synthesized by using Gaussian randomization method. Numerical simulation results demonstrate that the proposed method offer better performance than the state-of-the-art algorithms.

Keywords: MIMO radar; beampattern synthesis; one-bit quantization; waveform design

1 Introduction

Multiple-input multiple-output (MIMO) systems, as an emerging area, has been successfully applied in many fields, such as radar, sonar and wireless communication [1–4]. In particular, in recent years, MIMO radar becomes more attractive due to the extraordinary performance gain [5]. Compared with its conventional phased-array counterpart, MIMO radar can simultaneously emit multiple different signal waveforms from transmit antennas. Meanwhile, the receiver is able to capture those signals which are reflected from target(s) and interference(s). Therefore, how to improve the intensity of the backscattered signals from target(s) and suppress others is an essential problem for MIMO radar system. A strategy to tackle this problem is synthesizing a desired transmit waveform which can concentrate the radiated energy into the interested region(s), i.e., mainlobe(s). Leveraging on the advantage of multiple beams, MIMO radar expresses some fascinating features like better resolution capability [6], improved target detection performance [7] and flexible beampattern design [8, 9].

As a central task of MIMO radar, the transmit waveforms should be properly designed such that the transmit beampattern satisfies some predefined specification or criterion. By doing so, the received signal-to-interference-plus-noise ratio (SINR) can be enhanced. Generally speaking, the existing waveform optimization algorithms can be roughly classified into the following three cat-

Manuscript received Oct. 7, 2021; revised Nov. 20, 2021; accepted Nov. 26, 2021. The associate editor coordinating the review of this manuscript was Dr. Xiaofei Zhang. This work was supported by the National Natural Science Foundation of China (No.62171292) and the Guangdong Basic and Applied Basic Research Foundation (No. 2020A1515010410)

Tong Wei is with the Interdisciplinary Centre for Security, Reliability and Trust (SnT), University of Luxembourg, L-1855, Luxembourg.

Bin Liao is with the Guangdong Key Laboratory of Intelligent Information Processing, Shenzhen University, Shenzhen 518060, China.

✉ Corresponding author. Email: binliao@szu.edu.cn

DOI: 10.15918/j.jbit1004-0579.2021.067

egories: (i) minimization of the mean square error (MSE) between designed and desirable pattern, which is also known as match design [8–17]. (ii) joint design of the transmit waveform and receive filter via maximizing the output signal-to-interference-plus-noise ratio [18–24]. (iii) optimization of the emitted signals so as to maximize the radiated energy at the angle-of-interest (i.e., mainlobe region) and minimize it in elsewise (i.e., sidelobe region) [25–29]. For clear clarification, all of these categories will be introduced, respectively, in the sequel.

Exploiting the MMSE criterion, the matching design, which can be further divided into two branches, has been widely used to obtain a desirable pattern. A two-step method is first introduced to deal this problem in [8]. Through minimizing the difference between synthesized pattern and a desired one, the waveform covariance matrix is synthesized. Then, the real emitted waveform is achieved by decomposing the matrix. To achieve better match performance, in [14], a sparse representation based algorithm is proposed to obtain the cross-correlation matrix of signal. Similar to [8], the procedure of generating more practical waveform is still needed. Noticed that the second step is generally complex due to the nonconvexity of the decomposition problem especially with some waveform constraints. Hence, one-step method becomes more attractive even though its fourth-order objective. For example, in [12], the transmit signal is directly obtained by solving the unconstrained quadratic programming through Newton 's method. However, this method does not impose any practical constraints for transmitted signal and hence unsuitable for real system. Recently with this task, although imposing a constant modulus constraint (CMC), preferable transmit beampattern is still reached via complex circle manifold optimization [17]. Meanwhile, the resulting noconvex problem is tackled by projection, descent and retraction (PDR) algorithm. Note that these works only focus on the transmit end.

Considering the function of MIMO radar systems, jointly designing transmit waveform and receive filter, which involves maximizing the output signal-to-interference-plus-noise ratio (SINR), is generally preferred. To deal with this problem, in [20], an iterative algorithm, which guarantees a robust convergence property, is devised to maximize the output SINR under the requirements of similarity and constant modulus for radiated signals. For the same goal, a generalized majorization-minimization (MM) method is proposed in [22] to handle the problem of multiple waveform constraints. In [24], the design problem is first formulated as a nonconvex problem with fractional quadratic objective and several quadratic constraints. To solve this problem, an iterative algorithm, which combines minimum variance distortionless response (MVDR) and rank-one semidefinite relaxation (SDR) method, is devised. This method can obtain a better SINR than others.

The third category of waveform design dedicates to focus the radiated energy into mainlobe(s) and minimize it in sidelobe(s). On this basis, the transmit beamspace technique is developed in [25] through emitting orthogonal signal. Essentially, this method concentrates transmit energy by designing a multidimensional beamforming weight matrix and then a suboptimal solution for the resulting problem is obtained through eigenvalue decomposition (EVD). To describe the problem more accurately, the integrated sidelobe to mainlobe ratio (ISMR) of beampattern, which can be directly used to evaluate the performance of energy focusing, is introduced in [26]. Then the commercial solver, i.e., CVX [30], is utilized to solve the resulting semidefinite programming (SDP). In order to tackle steering vector mismatch and improve the robustness, a worst-case peak sidelobe level (PSL) optimization method is developed in [27]. Recently, under the coexist condition of MIMO radar and MIMO communication, the radar transmit waveform is synthesized to reduce inter-

ference for communication system as much as possible [29].

It should be noted that the high-resolution digital-to-analog converts (DACs), which cause massive circuit consumption and unacceptable hardware-cost, are required for all the aforementioned design methods. Hence, system with low-resolution, even one-bit, DACs have attracted much research interest [31-37]. For example, in [31] and [32], one-bit DACs are deployed for the transmit terminal of MIMO radar and the QPSK signal waveform is optimized to match a predefined pattern. In [38], the problem of transmit sequence design for a dual-function MIMO radar and communication system equipped with one-bit DACs has been addressed, two schemes, namely direct transmit sequence design and indirect transmit beamforming design, are devised to deal with the challenges introduced by the one-bit DACs. Different from the previous works [26, 32], in this paper, we attempt to design the MIMO radar transmit waveform with one-bit DACs by minimizing ISMR [39]. Specifically, the design problem is first recast as a constrained fractional quadratic problem (CFQP). Secondly, we utilize SDR technique to convert/relaxe the original nonconvex programming as convex SDP and further reduce the optimization complexity by tacking advantage of the special block-sparse structure. Lastly, a specialized interior point algorithm is devised to solve the resulting SDP. The main contributions of this work are listed as follows:

1) Following the optimization criterion of minimizing the ISMR of transmit beampattern, a nonconvex problem, which involves fractional quadratic objective and a set of discrete binary constraint (i.e., CFQP), is formulated.

2) Instead of directly solving the relaxed quasiconvex problem, we develop a block-sparse semidefinite relaxation (BSDR) method to covert it into a standard SDP and further reduce the size of optimization problem.

3) A specialized primal-dual interior point algorithm (IPA), which shows promising robustness and convergence performance, is proposed to tackle the reformulated low dimensional SDP.

4) Different simulation scenarios are considered to demonstrate the improved performance of our proposed algorithm over the state-of-the-art algorithms.

The rest of this paper is organized as follows. In Section 2, the signal model of MIMO radar with one-bit DACs and optimization problem formulation are first introduced. Next, in Section 3, a novel BSDR method is developed to tackle the problem of one-bit waveform design. The complexity and performance of our proposed algorithm is analyzed in Section 4. Then, a set of numerical simulations is arranged in Section 5. Finally, Section 6 draws the conclusions of this paper.

Notations: Vectors and matrices are denoted by lower case boldface letter and upper case boldface letter, respectively. Superscript $(\cdot)^{\mathrm{T}}$, $(\cdot)^*$ and $(\cdot)^{\mathrm{H}}$ denote the operation of transpose, conjugate, and Hermitian transpose, respectively. We denote by $\boldsymbol{I}$ the identity matrix and by $\mathbf{0}$ null matrix, respectively. $\boldsymbol{X} \succeq \mathbf{0}$ denotes a semidefinite matrix and $\otimes$ is the Kroneker product. $|\cdot|$ and $\|\cdot\|$ denote the absolute value and the l_2 norm, respectively. $\mathrm{j} = \sqrt{-1}$ is the imaginary unit. $\mathrm{Diag}(\boldsymbol{t})$ denotes a diagonal matrix with the diagonal elements given by the elements of $\boldsymbol{t}$. $\mathrm{vec}(\cdot)$ denotes the vectorization of a matrix, i.e., $\mathrm{vec}(\boldsymbol{X})$ is a column vector which stacks all the columns of $\boldsymbol{X}$ by vector form. $\mathrm{Re}(\cdot)$ and $\mathrm{Im}(\cdot)$ denote the real part and the imaginary part of complex matrix (or vector), respectively.

2 Signal Model and Problem Formulation

2.1 Signal Model

We consider a monostatic MIMO radar system with N transmit antennas, which are deployed as

a uniform linear array (ULA) with half-wavelength inter-element spacing. Each transmit antenna emits a different signal waveform $s_n(l)$ with $n=1,2,\cdots,N$ and $l=1,2,\cdots,L$, where L denotes the total number of discrete time samples within each signal pulse. Let $\boldsymbol{s}(l)\triangleq[s_1(l),s_2(l),\cdots,s_N(l)]\in\mathbb{C}^N$ be the transmit signal vector at the l-th time instant. In this paper, we consider the case where a pair of one-bit DACs are deployed for each channel to quantize the real and imaginary components of the complex signal, respectively. Therefore, the quantized waveform sequence, stacked by a vector form, can be expressed as follows

$$\boldsymbol{x}=[\boldsymbol{x}^{\mathrm{T}}(1),\cdots,\boldsymbol{x}^{\mathrm{T}}(L)]^{\mathrm{T}},\ \boldsymbol{x}(l)=\mathcal{Q}_c\big(\boldsymbol{s}(l)\big) \tag{1}$$

where $\mathcal{Q}_c(\cdot)=\mathcal{Q}(\cdot)+\mathrm{j}\mathcal{Q}(\cdot)$ denotes the element-wise complex-value one-bit quantizer. For simplicity, the threshold of each real-value quantizer is specified as zero value and hence we have

$$\mathcal{Q}(s)=\begin{cases}+\alpha, s\in[0,+\infty]\\ -\alpha, s\in[-\infty,0)\end{cases} \tag{2}$$

where s denotes arbitrary real number and $\alpha>0$ is related to the transmit power. Meanwhile, the total transmit power, which denoted by E, satisfies the following condition:

$$\|\boldsymbol{x}\|^2=\sum_{l=1}^{L}\|\boldsymbol{x}(l)\|^2=E \tag{3}$$

Substituting (2) into (1) and recalling (3), it can be immediately concluded that $\alpha=\sqrt{\dfrac{E}{2NL}}$ and $\boldsymbol{x}$ belongs the following QPSK constellation

$$\mathcal{X}=\{\pm\alpha\pm\mathrm{j}\alpha\} \tag{4}$$

Assuming the emitted signals are narrowband, the synthesized signal at the target direction θ, which belongs to the whole spatial angle set Θ, can be expressed as

$$\begin{aligned}\boldsymbol{y}(\theta)=&[\boldsymbol{a}^{\mathrm{T}}(\theta)\boldsymbol{x}(1),\boldsymbol{a}^{\mathrm{T}}(\theta)\boldsymbol{x}(2),\cdots,\boldsymbol{a}^{\mathrm{T}}(\theta)\boldsymbol{x}(L)]^{\mathrm{T}}=\\ &(\boldsymbol{I}_L\otimes\boldsymbol{a}^{\mathrm{T}}(\theta))\boldsymbol{x}\end{aligned} \tag{5}$$

where $\boldsymbol{a}(\theta)\in\mathbb{C}^N$ denotes the transmit steering vector which can be written as follows

$$\boldsymbol{a}(\theta)=[1,\mathrm{e}^{-\mathrm{j}\pi\sin(\theta)},\cdots,\mathrm{e}^{-\mathrm{j}\pi(N-1)\sin(\theta)}]^{\mathrm{T}} \tag{6}$$

According to (5), the transmit beampattern which can be characterized by the spatial power spectrum is expressed as follows [28]

$$\begin{aligned}P(\theta)=&\boldsymbol{y}^{\mathrm{H}}(\theta)\boldsymbol{y}(\theta)=\\ &\sum_{l=1}^{L}|\boldsymbol{a}^{\mathrm{T}}(\theta)\boldsymbol{x}(l)|^2=\\ &\boldsymbol{x}^{\mathrm{H}}(\boldsymbol{I}_L\otimes\boldsymbol{a}^{*}(\theta)\boldsymbol{a}^{\mathrm{T}}(\theta))\boldsymbol{x}\end{aligned} \tag{7}$$

2.2 Problem Formulation

Generally speaking, the transmit signal waveform $\boldsymbol{x}\in\mathbb{C}^{NL}$ is desired to be properly synthesized such that the available transmit energy can be concentrated into the mainlobe region Θ_m as much as possible. Noted that Θ_m may consist of several sub-regions. Consequently, from (7), the integrated sidelobe to mainlobe ratio (ISMR) of transmit beampattern, which can be used to evaluate the quality of energy focusing, is defined as [26]

$$\begin{aligned}\mathrm{ISMR}=&\frac{\int_{\Theta_s}\boldsymbol{x}^{\mathrm{H}}(\boldsymbol{I}_L\otimes\boldsymbol{a}^{*}(\theta)\boldsymbol{a}^{\mathrm{T}}(\theta))\boldsymbol{x}\mathrm{d}\theta}{\int_{\Theta_m}\boldsymbol{x}^{\mathrm{H}}(\boldsymbol{I}_L\otimes\boldsymbol{a}^{*}(\theta)\boldsymbol{a}^{\mathrm{T}}(\theta))\boldsymbol{x}\mathrm{d}\theta}=\\ &\frac{\boldsymbol{x}^{\mathrm{H}}\boldsymbol{\Upsilon}_s\boldsymbol{x}}{\boldsymbol{x}^{\mathrm{H}}\boldsymbol{\Upsilon}_m\boldsymbol{x}}\end{aligned} \tag{8}$$

where Θ_s denotes the sidelobe region, $\boldsymbol{\Upsilon}_s$ and $\boldsymbol{\Upsilon}_m$ are defined, respectively, as

$$\boldsymbol{\Upsilon}_s=\boldsymbol{I}_L\otimes\boldsymbol{A}(\Theta_s),\ \ \boldsymbol{\Upsilon}_m=\boldsymbol{I}_L\otimes\boldsymbol{A}(\Theta_m) \tag{9}$$

and the integral $\boldsymbol{A}(\Theta)\triangleq\int_{\Theta}\boldsymbol{a}^{*}(\theta)\boldsymbol{a}^{\mathrm{T}}(\theta)\mathrm{d}\theta$ over Θ (either Θ_m or Θ_s) can be numerically computed. For notation simplicity, the $\boldsymbol{A}(\Theta_s)$ and $\boldsymbol{A}(\Theta_m)$ are denoted as $\boldsymbol{A}_s$ and $\boldsymbol{A}_m$, respectively, in what follows. According to (9), it is noticed that both $\boldsymbol{\Upsilon}_s$ and $\boldsymbol{\Upsilon}_m$ are composed of a diagonal block-sparse matrix. By sufficiently taking advantage of this special structure, the formulated optimization problem size will be greatly reduced. Thereby, compared with its existing counterpart, the computational efficiency of our algorithm can be significantly improved.

To focus the transmit energy into mainlobe region, the ISMR is expected to be minimized by selecting an appropriate waveform sequence $\boldsymbol{x}$ from the predefined alphabet set $\mathcal{X}$. Keeping the above requirements in mind, mathematically, the

following optimization problem can be formulated

$$\begin{aligned} \min_{\boldsymbol{x}} \quad & \frac{\boldsymbol{x}^{\mathrm{H}}\boldsymbol{\Upsilon}_s\boldsymbol{x}}{\boldsymbol{x}^{\mathrm{H}}\boldsymbol{\Upsilon}_m\boldsymbol{x}} \\ \text{s.t.} \quad & \boldsymbol{x}\in\mathcal{X} \end{aligned} \tag{10}$$

which is, however, difficult to tackle due to the quadratic fractional objective and discrete constraint. Toward this end, the block-sparse semidefinite relaxation (BSDR) based algorithm will be introduced to deal with problem (10) in the sequel.

3 The Proposed BSDR-Based Algorithm

Since the CFQP (10) is generally NP-hard [40, 41], there is not polynomial time algorithm to guarantee a globally optimal solution. Theoretically, we can use exhaustive search to solve the problem (10). However, in this scenario, the computational complexity is impractical especially in large-scale data regimes, e.g., existing 10^3–10^4 complex variables in our consideration. Toward this end, we first utilize the semidefinite relaxation (SDR) technique to approximate the optimal solution of the problem (10). Besides, the dimension of relaxed problem, which determines the overall operation time, is further reduced by exploiting the advantage of special block-sparse structure expressed as (9). Thereby, we nominate the novel QPSK waveform design approach for MIMO radar as BSDR algorithm. With the synthesized waveform correlation, the one-bit Gaussian randomization method is used to obtain the desired one-bit waveform sequence directly.

3.1 The Block-sparse SDR-based Algorithm for (10)

In order to facilitate the development of the algorithm, the problem (10) is first transformed into the corresponding real-value form expressed as follows

$$\begin{aligned} \min_{\boldsymbol{x}_r} \quad & \frac{\boldsymbol{x}_r^{\mathrm{T}}\boldsymbol{\Upsilon}_{s,r}\boldsymbol{x}_r}{\boldsymbol{x}_r^{\mathrm{T}}\boldsymbol{\Upsilon}_{m,r}\boldsymbol{x}_r} \\ \text{s.t.} \quad & \boldsymbol{x}_r\in\mathcal{X}_r \end{aligned} \tag{11}$$

where $\boldsymbol{x}_r=[\mathrm{Re}\{\boldsymbol{x}\}^{\mathrm{T}},\mathrm{Im}\{\boldsymbol{x}\}^{\mathrm{T}}]^{\mathrm{T}}$ denotes the emitted one-bit waveform sequence, $\mathcal{X}_r=\{\pm\alpha\}$,

$$\boldsymbol{\Upsilon}_{s,r}=\begin{bmatrix}\mathrm{Re}\{\boldsymbol{\Upsilon}_s\} & -\mathrm{Im}\{\boldsymbol{\Upsilon}_s\}\\ \mathrm{Im}\{\boldsymbol{\Upsilon}_s\} & \mathrm{Re}\{\boldsymbol{\Upsilon}_s\}\end{bmatrix} \tag{12}$$

and $\boldsymbol{\Upsilon}_{m,r}$ is similarly defined.

Let us introduce a real matrix $\boldsymbol{X}=\boldsymbol{x}_r\boldsymbol{x}_r^{\mathrm{T}}\in\mathbb{R}^{2NL\times 2NL}$, the binary optimization problem (11) can then be equivalently rewritten as

$$\begin{aligned} \min_{\boldsymbol{x}_r,\boldsymbol{X}} \quad & \frac{\mathrm{Tr}(\boldsymbol{\Upsilon}_{s,r}\boldsymbol{X})}{\mathrm{Tr}(\boldsymbol{\Upsilon}_{m,r}\boldsymbol{X})} \\ \text{s.t.} \quad & \boldsymbol{X}=\boldsymbol{x}_r\boldsymbol{x}_r^{\mathrm{T}} \\ & \boldsymbol{x}_r\in\mathcal{X}_r \end{aligned} \tag{13}$$

Proposition 1 The feasible set of problem (13) can be equivalently expressed as follows: $\boldsymbol{X}\succeq\boldsymbol{0}$, $\mathrm{rank}(\boldsymbol{X})=1$ and $[\boldsymbol{X}]_{i,i}=\alpha^2,\forall i\in\mathcal{I}$, where $[\boldsymbol{X}]_{i,i}$ denotes the i-th diagonal entry of $\boldsymbol{X}$ and $\mathcal{I}=\{1,2,\cdots,2NL\}$.

Proof Firstly, we consider to prove the sufficiency. For any real-value vector $\boldsymbol{x}_r$, we always have the generalized inequality $\boldsymbol{x}_r\boldsymbol{x}_r^{\mathrm{T}}\succeq\boldsymbol{0}$. Recalling that $\boldsymbol{X}=\boldsymbol{x}_r\boldsymbol{x}_r^{\mathrm{T}}$ and $\boldsymbol{x}_r\in\mathcal{X}_r$, we can immediately conclude that $\boldsymbol{X}\succeq\boldsymbol{0}$, $\mathrm{rank}(\boldsymbol{X})=1$ and $[\boldsymbol{X}]_{i,i}=\alpha^2,\forall i\in\mathcal{I}$. Next, we continue to prove the necessity. Let us perform the eigenvalue decomposition (EVD) for $\boldsymbol{X}$ as follows: $\boldsymbol{X}=\boldsymbol{U}\boldsymbol{\Lambda}\boldsymbol{U}^{\mathrm{T}}$ where $\boldsymbol{U}=[\boldsymbol{u}_1,\boldsymbol{u}_2,\cdots,\boldsymbol{u}_{2NL}]$ and $\boldsymbol{\Lambda}=\mathrm{diag}[\lambda_1,\lambda_2,\cdots,\lambda_{2NL}]$ denote the corresponding eigenvector and eigenvalue, respectively. Through the $\mathrm{rank}(\boldsymbol{X})=1$ constraint, one can immediately obtain $\boldsymbol{X}=\lambda_1\boldsymbol{u}_1\boldsymbol{u}_1^{\mathrm{T}}$ where λ_1 and $\boldsymbol{u}_1$ denote the principle eigenvalue and eigenvector, respectively. Recalling that $[\boldsymbol{X}]_{i,i}=\alpha^2,\forall i\in\mathcal{I}$, we can conclude that $\mathrm{Tr}(\boldsymbol{X})=\lambda_1\|\boldsymbol{u}_1\|^2=\lambda_1=E$ and hence each entries of $\boldsymbol{u}_1$ should be strictly equal to $\pm\sqrt{\frac{1}{2NL}}$. Noticed that $\lambda_1\geq 0$ due to $\boldsymbol{X}\succeq\boldsymbol{0}$. Thus, we can let $\boldsymbol{x}_r=\sqrt{\lambda_1}\boldsymbol{u}_1\in\mathcal{X}_r$ and further conclude $\boldsymbol{X}=\boldsymbol{x}_r\boldsymbol{x}_r^{\mathrm{T}}$. The proof is completed.

According to Proposition 1, the problem (13) can be recast as

$$\begin{aligned} \min_{\boldsymbol{X}} \quad & \frac{\mathrm{Tr}(\boldsymbol{\Upsilon}_{s,r}\boldsymbol{X})}{\mathrm{Tr}(\boldsymbol{\Upsilon}_{m,r}\boldsymbol{X})} \\ \text{s.t.} \quad & \boldsymbol{X} \succeq \boldsymbol{0} \\ & \mathrm{rank}(\boldsymbol{X}) = 1 \\ & [\boldsymbol{X}]_{i,i} = \alpha^2,\ \forall i \in \mathcal{I} \end{aligned} \tag{14}$$

It can be observed that the rank constraint in (14) is nonconvex and hence difficult to tackle. To overcome this issue, we employ the SDR technique to approximate the problem (11) by dropping the rank constraint [42]. By doing so, the corresponding relaxation of problem (14) can be expressed as

$$\begin{aligned} \min_{\boldsymbol{X}} \quad & \frac{\mathrm{Tr}(\boldsymbol{\Upsilon}_{s,r}\boldsymbol{X})}{\mathrm{Tr}(\boldsymbol{\Upsilon}_{m,r}\boldsymbol{X})} \\ \text{s.t.} \quad & \boldsymbol{X} \succeq \boldsymbol{0} \\ & [\boldsymbol{X}]_{i,i} = \alpha^2,\ \forall i \in \mathcal{I} \end{aligned} \tag{15}$$

whose globally optimal solution is denoted by $\boldsymbol{X}^\star$.

Notice that the problem (15) is a quasi-convex problem on account of linear fractional objective function. In general, a nearly globally optimal solution for this kind of problem can be acquired by the classical bisection method [40], but more computational burden is caused when solving the problem. Meanwhile, the accuracy of solution is greatly depend on the time of bisection. To this end, we can further convert quasi-convex problem (15) into its convex counterpart expressed as follows [43, 44]

$$\begin{aligned} \min_{\boldsymbol{W} \in \mathbb{R}^{2NL \times 2NL}} \quad & \mathrm{Tr}(\boldsymbol{\Upsilon}_{s,r}\boldsymbol{W}) \\ \text{s.t.} \quad & \mathrm{Tr}(\boldsymbol{\Upsilon}_{m,r}\boldsymbol{W}) = 1 \\ & \boldsymbol{W} \succeq \boldsymbol{0} \\ & [\boldsymbol{W}]_{2NL,2NL} = [\boldsymbol{W}]_{j,j} \end{aligned} \tag{16}$$

where $j = 1, 2, \cdots, 2NL-1$ and $\boldsymbol{W} = \boldsymbol{X}/\mathrm{Tr}(\boldsymbol{\Upsilon}_{m,r}\boldsymbol{X})$. Similarly, the globally optimal solution of (16) is denoted by $\boldsymbol{W}^\star$. The correlation between $\boldsymbol{W}^\star$ and $\boldsymbol{X}^\star$ will be discussed in what follows.

$$\boldsymbol{W} = \begin{bmatrix} W_{1,1} & \cdots & W_{1,L} & W_{1,L+1} & \cdots & W_{1,2L} \\ \vdots & \ddots & \vdots & \vdots & \ddots & \vdots \\ W_{L,1} & \cdots & W_{L,L} & W_{L,L+1} & \cdots & W_{L,2L} \\ W_{L+1,1} & \cdots & W_{L+1,L} & W_{L+1,L+1} & \cdots & W_{L+1,2L} \\ \vdots & \ddots & \vdots & \vdots & \ddots & \vdots \\ W_{2L,1} & \cdots & W_{2L,L} & W_{2L,L+1} & \cdots & W_{2L,2L} \end{bmatrix} \tag{17}$$

Proposition 2 The linear fraction quasi-convex problem (15) exists the same optimal objective value as its convex counterpart (16). Meanwhile, the optimum solution of (15) can be obtained from the equation: $\boldsymbol{X}^\star = \alpha^2\boldsymbol{W}^\star/[\boldsymbol{W}^\star]_{i,i}$, $\forall i \in \mathcal{I}$.

Proof The main idea of this proof follows the Proposition 1 in [27]. We assume that $\boldsymbol{W}$ is any feasible solution of (16). It is easy concluded that the corresponding point $\widetilde{\boldsymbol{X}} = \alpha^2\boldsymbol{W}/[\boldsymbol{W}]_{i,i}$ is also feasible for problem (15) and exists the same objective value $\mathrm{Tr}(\boldsymbol{\Upsilon}_{s,r}\widetilde{\boldsymbol{X}})/\mathrm{Tr}(\boldsymbol{\Upsilon}_{m,r}\widetilde{\boldsymbol{X}}) = \mathrm{Tr}(\boldsymbol{\Upsilon}_{s,r}\boldsymbol{W})$. On the other hand, we recall the Charnes-Coopper transformation $\widetilde{\boldsymbol{W}} = \boldsymbol{X}/\mathrm{Tr}(\boldsymbol{\Upsilon}_{m,r}\boldsymbol{X})$, where $\boldsymbol{X}$ is similarly defined as the feasible solution of (15). We can also see that $\widetilde{\boldsymbol{W}}$ is feasible for problem (16) and has the same objective value $\mathrm{Tr}(\boldsymbol{\Upsilon}_{s,r}\widetilde{\boldsymbol{W}}) = \mathrm{Tr}(\boldsymbol{\Upsilon}_{s,r}\boldsymbol{X})/\mathrm{Tr}(\boldsymbol{\Upsilon}_{m,r}\boldsymbol{X})$. Based on above, we conclude that problem (15) and (16) are equivalent and $\boldsymbol{X}^\star = \alpha^2\boldsymbol{W}^\star/[\boldsymbol{W}^\star]_{i,i}, \forall i \in \mathcal{I}$. The proof is completed.

Despite the complex fractional quadratic problem (11) with binary constraint has been converted into its convex counterpart (16). However, even though its convexity, it is still challenging to directly solve the SDP (16) on account of large-scale problem size (i.e., with 10^3–10^4 variables in our consideration). Thereby, exploiting the special block-sparse structure of our problem, we can further simplify our algorithm via greatly reducing the dimension of optimization problem (i.e., with 10-10^2 variables in reduced scenario). Let us partition $\boldsymbol{W}$ into $2L \times 2L$ blocks as the manner of (17) which arranged at the top of this page.

Lemma 1 The objective function and first con-

straint of problem (16) can be expressed as follows:

$$\mathrm{Tr}(\boldsymbol{\Upsilon}_{s,r}\boldsymbol{W}) = \sum_{l=1}^{L}\mathrm{Tr}\left(\boldsymbol{A}_{s,r}\boldsymbol{W}_l\right) \tag{18a}$$

$$\mathrm{Tr}(\boldsymbol{\Upsilon}_{m,r}\boldsymbol{W}) = \sum_{l=1}^{L}\mathrm{Tr}\left(\boldsymbol{A}_{m,r}\boldsymbol{W}_l\right) = 1 \tag{18b}$$

where

$$\boldsymbol{W}_l = \begin{bmatrix} \boldsymbol{W}_{l,l} & \boldsymbol{W}_{l,L+l} \\ \boldsymbol{W}_{L+l,l} & \boldsymbol{W}_{L+l,L+l} \end{bmatrix} \tag{19a}$$

$$\boldsymbol{A}_{s,r} = \begin{bmatrix} \mathrm{Re}\{\boldsymbol{A}_s\} & -\mathrm{Im}\{\boldsymbol{A}_s\} \\ \mathrm{Im}\{\boldsymbol{A}_s\} & \mathrm{Re}\{\boldsymbol{A}_s\} \end{bmatrix} \tag{19b}$$

and $\boldsymbol{A}_{m,r}$ is similarly defined as (19b).

Proof See Appendix **A**.

According to Lemma 1, it is observed that the objective function of problem (16) is composed of cumulative L terms. Consequently, we first optimize one of the variable (i.e., $\boldsymbol{W}_l$) with its corresponding constraint. After that, let all of variables are equal to it.

By doing so, the problem (16) can be simplified as

$$\begin{aligned} \min_{\boldsymbol{W}\in\mathbb{R}^{2N\times 2N}} \quad & \mathrm{Tr}(\boldsymbol{A}_{s,r}\boldsymbol{W}) \\ \text{s.t.} \quad & \mathrm{Tr}(\boldsymbol{A}_{m,r}\boldsymbol{W}) = \frac{1}{L} \\ & \boldsymbol{W} \succeq \boldsymbol{0} \\ & [\boldsymbol{W}]_{2N,2N} = [\boldsymbol{W}]_{i,i} \end{aligned} \tag{20}$$

where $i = 1, 2, \cdots, 2N-1$. Let us denote the globally optimal solution of (20) as $\boldsymbol{W}^{\star}$. It is noticed that reduced semidefinite programming (SDP) problem (20) exists relative interior point to meet all the constraints and hence the strong duality hold [28]. Therefore, the primal-dual interior point algorithm (IPA), which is the most robust and widely used algorithm for general SDP, can be utilized to tackle problem (20) efficiently. On the other hand, despite that the convex problem (20) can be solved by the popular commercial SDP solvers such as SeDuMi [45] and CVX [30], we still dedicate to designing a specialized IPA to give some insights and further enhance the computational efficiency for the simplified problem (20).

The dual semidefinite programming (DSDP) of problem (33) can be easily derived as

$$\begin{aligned} \max_{y,\boldsymbol{t},\boldsymbol{Z}} \quad & \frac{y}{L} \\ \text{s.t.} \quad & y \in \mathbb{R}, \boldsymbol{t} \in \mathbb{R}^{2N-1}, \boldsymbol{Z} \in \mathbb{R}^{2N\times 2N} \\ & \boldsymbol{Z} \succeq \boldsymbol{0} \\ & \boldsymbol{A}_{s,r} - \boldsymbol{Z} - y\boldsymbol{A}_{m,r} + \mathrm{Diag}\begin{pmatrix} -\boldsymbol{t} \\ \boldsymbol{e}^{\mathrm{T}}\boldsymbol{t} \end{pmatrix} = \boldsymbol{0} \end{aligned} \tag{21}$$

where $(y, \boldsymbol{t}, \boldsymbol{Z})$ are consist of the dual variables of primal SDP problem (20), $\boldsymbol{e}$ denotes all-one vector with dimension $2N-1$. Meanwhile, the associated logarithmetic barrier dual problem (BDP) of (21) is given by [46]

$$\begin{aligned} \max_{y,\boldsymbol{t},\boldsymbol{Z}} \quad & \frac{y}{L} + \mu\log\det(\boldsymbol{Z}) \\ \text{s.t.} \quad & y \in \mathbb{R}, \boldsymbol{t} \in \mathbb{R}^{2N-1}, \boldsymbol{Z} \in \mathbb{R}^{2N\times 2N} \\ & \boldsymbol{Z} \succeq \boldsymbol{0} \\ & \boldsymbol{A}_{s,r} - \boldsymbol{Z} - y\boldsymbol{A}_{m,r} + \mathrm{Diag}\begin{pmatrix} -\boldsymbol{t} \\ \boldsymbol{e}^{\mathrm{T}}\boldsymbol{t} \end{pmatrix} = \boldsymbol{0} \end{aligned} \tag{22}$$

where μ is a positive real number called the barrier parameter. It is easily observed that (22) approximates (21) as $\mu \to 0$. Hence, we can update μ in a monotonic decrease method.

To further describe our specialized IPA, the Lagrangian function associated with the BDP (22) is expressed as

$$\begin{aligned} &\mathcal{L}(\boldsymbol{W}, y, \boldsymbol{t}, \boldsymbol{Z}) = \frac{y}{L} + \mu\log\det(\boldsymbol{Z}) + \\ &\mathrm{Tr}\left(\left(\boldsymbol{A}_{s,r} - \boldsymbol{Z} - y\boldsymbol{A}_{m,r} + \mathrm{Diag}\begin{pmatrix} -\boldsymbol{t} \\ \boldsymbol{e}^{\mathrm{T}}\boldsymbol{t} \end{pmatrix}\right)\boldsymbol{W}\right), \\ &\boldsymbol{Z} \succeq \boldsymbol{0}, \boldsymbol{W} \succeq \boldsymbol{0} \end{aligned} \tag{23}$$

Consequently, the first-order optimality conditions for the saddle point of this Lagrangian are easily derived as follows

$$\nabla_{\boldsymbol{W}}\mathcal{L} = \boldsymbol{A}_{s,r} - \boldsymbol{Z} - y\boldsymbol{A}_{m,r} + \mathrm{Diag}\begin{pmatrix} -\boldsymbol{t} \\ \boldsymbol{e}^{\mathrm{T}}\boldsymbol{t} \end{pmatrix} = \boldsymbol{0} \tag{24a}$$

$$\nabla_{y}\mathcal{L} = \frac{1}{L} - \mathrm{Tr}(\boldsymbol{A}_{m,r}\boldsymbol{W}) = 0 \tag{24b}$$

$$\nabla_{\boldsymbol{t}}\mathcal{L} = \begin{bmatrix} \mathrm{Tr}(\boldsymbol{J}_1\boldsymbol{W}) \\ \vdots \\ \mathrm{Tr}(\boldsymbol{J}_K\boldsymbol{W}) \end{bmatrix} = \boldsymbol{0} \tag{24c}$$

$$\nabla_{\boldsymbol{Z}}\mathcal{L} = \mu\boldsymbol{Z}^{-1} - \boldsymbol{W} = \boldsymbol{0}, \boldsymbol{Z} \succeq \boldsymbol{0}, \boldsymbol{W} \succeq 0 \tag{24d}$$

where $\boldsymbol{J}_k \in \mathbb{R}^{2N\times 2N}, k = 1, \cdots, 2N-1$ denotes the diagonal matrix which k-th and $2N$-th diagonal

element are consist of -1 and $+1$, respectively, with the others are 0. It is noted that equation (24a)– (24d) compose the Karush-Kuhn-Tucker (KKT) conditions for DBP (22). Hence, the solution of linear system (24) which denotes by $(\boldsymbol{W}^\star, y^\star, \boldsymbol{t}^\star, \boldsymbol{Z}^\star)$ is optimal solution for problem (22). When μ becomes small enough, the equations (24) is also the equivalent KKT conditions for DSDP (21) and hence SDP (20).

In order to find the direction $(\Delta\boldsymbol{W}, \Delta y, \Delta\boldsymbol{t}, \Delta\boldsymbol{Z})$ toward optimal solution, we can utilize Newton's Method with conditions

$$\Delta\boldsymbol{Z}+\Delta y\boldsymbol{A}_{m,r}-\mathrm{Diag}\begin{pmatrix}-\Delta\boldsymbol{t}\\ \boldsymbol{e}^{\mathrm{T}}\Delta\boldsymbol{t}\end{pmatrix}=R_d \tag{25a}$$

$$\begin{bmatrix}\mathrm{Tr}(\boldsymbol{A}_{m,r}\Delta\boldsymbol{W})\\ \mathrm{Tr}(\boldsymbol{J}_1\Delta\boldsymbol{W})\\ \vdots\\ \mathrm{Tr}(\boldsymbol{J}_K\Delta\boldsymbol{W})\end{bmatrix}=r_p \tag{25b}$$

$$\Delta\boldsymbol{Z}\boldsymbol{W}+\boldsymbol{Z}\Delta\boldsymbol{W}=R_c \tag{25c}$$

where R_d, r_p and R_c are defined, respectively, as

$$R_d \triangleq \boldsymbol{A}_{s,r}-\boldsymbol{Z}-y\boldsymbol{A}_{m,r}+\mathrm{Diag}\begin{pmatrix}-\boldsymbol{t}\\ \boldsymbol{e}^{\mathrm{T}}\boldsymbol{t}\end{pmatrix} \tag{26a}$$

$$r_p \triangleq -\begin{bmatrix}\mathrm{Tr}(\boldsymbol{A}_{m,r}\boldsymbol{W})-\frac{1}{L}\\ \mathrm{Tr}(\boldsymbol{J}_1\boldsymbol{W})\\ \vdots\\ \mathrm{Tr}(\boldsymbol{J}_K\boldsymbol{W})\end{bmatrix} \tag{26b}$$

$$R_c \triangleq \mu\boldsymbol{I}-\boldsymbol{Z}\boldsymbol{W} \tag{26c}$$

To tackle the linear system (25) simply, we can reformulate it as follows:

$$\mathrm{vec}(\Delta\boldsymbol{Z})+\Delta y\cdot\mathrm{vec}(\boldsymbol{A}_{m,r})-\boldsymbol{M}\Delta\boldsymbol{t}=r_d \tag{27a}$$

$$\begin{bmatrix}\mathrm{vec}^{\mathrm{T}}(\boldsymbol{A}_{m,r})\cdot\mathrm{vec}(\Delta\boldsymbol{W})\\ \mathrm{vec}^{\mathrm{T}}(\boldsymbol{J}_1)\cdot\mathrm{vec}(\Delta\boldsymbol{W})\\ \vdots\\ \mathrm{vec}^{\mathrm{T}}(\boldsymbol{J}_K)\cdot\mathrm{vec}(\Delta\boldsymbol{W})\end{bmatrix}=r_p \tag{27b}$$

$$(\boldsymbol{W}\otimes\boldsymbol{I})\mathrm{vec}(\Delta\boldsymbol{Z})+(\boldsymbol{I}\otimes\boldsymbol{Z})\mathrm{vec}(\Delta\boldsymbol{W})=r_c \tag{27c}$$

where $r_d=\mathrm{vec}(R_d)$, $r_c=\mathrm{vec}(R_c)$ and the selection matrix $\boldsymbol{M}=[\mathrm{vec}(\boldsymbol{J}_1),\cdots,\mathrm{vec}(\boldsymbol{J}_K)]$. For notation simplicity, we define $\boldsymbol{E}=(\boldsymbol{I}\otimes\boldsymbol{Z})$ and $\boldsymbol{F}=(\boldsymbol{W}\otimes\boldsymbol{I})$. Next, we can compactly rewrite (27) as

$$\begin{bmatrix}\boldsymbol{0} & \boldsymbol{G}^T & \boldsymbol{I}_{4N^2}\\ \boldsymbol{G} & \boldsymbol{0} & \boldsymbol{0}\\ \boldsymbol{E} & \boldsymbol{0} & \boldsymbol{F}\end{bmatrix}\begin{bmatrix}\mathrm{vec}(\Delta\boldsymbol{W})\\ \Delta\boldsymbol{t}_y\\ \mathrm{vec}(\Delta\boldsymbol{Z})\end{bmatrix}=\begin{bmatrix}r_d\\ r_p\\ r_c\end{bmatrix} \tag{28}$$

where $\boldsymbol{G}=[\mathrm{vec}(\boldsymbol{A}_{m,r}),-\boldsymbol{M}]^{\mathrm{T}}$ and $\Delta\boldsymbol{t}_y=[\Delta y,\Delta\boldsymbol{t}^{\mathrm{T}}]^{\mathrm{T}}$.

From (28), it is seen that

$$\boldsymbol{G}^{\mathrm{T}}\Delta\boldsymbol{t}_y+\mathrm{vec}(\Delta\boldsymbol{Z})=r_d \tag{29a}$$

$$\boldsymbol{E}\cdot\mathrm{vec}(\Delta\boldsymbol{W})+\boldsymbol{F}\cdot\mathrm{vec}(\Delta\boldsymbol{Z})=r_c \tag{29b}$$

By substituting the transformed (29b) into (29a), we have

$$\boldsymbol{G}^{\mathrm{T}}\Delta\boldsymbol{t}_y-\boldsymbol{F}^{-1}\boldsymbol{E}\cdot\mathrm{vec}(\Delta\boldsymbol{W})=r_d-\boldsymbol{F}^{-1}r_c \tag{30}$$

Applying the block Gaussian elimination, the system (28) can be reduced as [35]

$$\begin{bmatrix}-\boldsymbol{F}^{-1}\boldsymbol{E} & \boldsymbol{G}^{\mathrm{T}}\\ \boldsymbol{G} & \boldsymbol{0}\end{bmatrix}\begin{bmatrix}\mathrm{vec}\,(\Delta\boldsymbol{W})\\ \Delta\boldsymbol{t}_y\end{bmatrix}=\begin{bmatrix}r_d-\boldsymbol{F}^{-1}r_c\\ r_p\end{bmatrix} \tag{31}$$

Then, utilizing the second step of block Gaussian elimination to vanish $\mathrm{vec}(\Delta\boldsymbol{W})$, it is immediately derived that

$$\Delta\boldsymbol{t}_y=(\boldsymbol{G}\boldsymbol{E}^{-1}\boldsymbol{F}\boldsymbol{G}^{\mathrm{T}})^{-1}(r_p+\boldsymbol{G}\boldsymbol{E}^{-1}(\boldsymbol{F}r_d-r_c)) \tag{32}$$

Inserting this back into (29a) and (30), respectively, we have

$$\mathrm{vec}(\Delta\boldsymbol{Z})=r_d-\boldsymbol{G}^{\mathrm{T}}\Delta\boldsymbol{t}_y \tag{33a}$$

$$\mathrm{vec}(\Delta\boldsymbol{W})=\boldsymbol{E}^{-1}(\boldsymbol{F}(\boldsymbol{G}^{\mathrm{T}}\Delta\boldsymbol{t}_y-r_d)+r_c) \tag{33b}$$

Based on above discussions, we can reconstruct the directions $(\Delta\boldsymbol{W}, \Delta y, \Delta\boldsymbol{t}, \Delta\boldsymbol{Z})$ from (32), (33a) and (33b).

When the desired update directions are determined, we would like to step current point toward the new point $(\boldsymbol{W}+\Delta\boldsymbol{W}, y+\Delta y, \boldsymbol{t}+\Delta\boldsymbol{t}, \boldsymbol{Z}+\Delta\boldsymbol{Z})$ except that it violates the nonnegativity of $\boldsymbol{W}$ and $\boldsymbol{Z}$. Hence, the line search scheme can be used to find a proper update step-size $\alpha_p, \alpha_d \in (0,1]$ to keep the nonnegativity. Then, we step to the new point

$$\begin{cases}\boldsymbol{W}\Leftarrow\boldsymbol{W}+\alpha_p\Delta\boldsymbol{W}\\ y\Leftarrow y+\alpha_d\Delta y\\ \boldsymbol{t}\Leftarrow\boldsymbol{t}+\alpha_d\Delta\boldsymbol{t}\\ \boldsymbol{Z}\Leftarrow\boldsymbol{Z}+\alpha_d\Delta\boldsymbol{Z}\end{cases} \tag{34}$$

Finally, we can decreasingly update barrier parameter $\mu=0.5\times\mathrm{Tr}(\boldsymbol{W}\boldsymbol{Z})/2N$. Our algorithm re-

peats until the current point $(\boldsymbol{W}, y, \boldsymbol{t}, \boldsymbol{Z})$ satisfies both in terms of primal feasibility and dual feasibility, at the same time, the duality gap becomes small enough. According to the above descriptions, the proposed specialized primal-dual IPA for solving the SDP (20) is summarized in Algorithm 1.

Algorithm 1 Specialized IPA for primal SDP (20)

Input: $\boldsymbol{A}_{s,r}$, $\boldsymbol{A}_{m,r}$, N and L.

1: Set a strictly primal-dual feasible initial point $(\boldsymbol{W}, y, \boldsymbol{t}, \boldsymbol{Z})$ and a solution accuracy $\epsilon > 0$.

2: **repeat**

3: Set $\mu = 0.5 \times \dfrac{\mathrm{Tr}(\boldsymbol{W}\boldsymbol{Z})}{2N}$.

4: Compute the search direction $(\Delta y, \Delta \boldsymbol{t})$ from (32).

5: Compute $\mathrm{vec}(\Delta \boldsymbol{Z})$ from (33a) and then reconstruct the search direction $\Delta \boldsymbol{Z}$.

6: Compute $\mathrm{vec}(\Delta \boldsymbol{W})$ from (33b) and then reconstruct the search direction $\Delta \boldsymbol{W}$.

7: Use the line search to find the primal step-size $\alpha_p \in (0, 1]$ such that $\boldsymbol{W} \succeq \boldsymbol{0}$.

8: Use the line search to find the dual step-size $\alpha_d \in (0, 1]$ such that $\boldsymbol{Z} \succeq \boldsymbol{0}$.

9: Update the primal variable step toward the new point:

$$\boldsymbol{W} \Leftarrow \boldsymbol{W} + \alpha_p \Delta \boldsymbol{W}.$$

10: Update the dual variables step toward the new point:

$$y \Leftarrow y + \alpha_d \Delta y, \boldsymbol{t} \Leftarrow \boldsymbol{t} + \alpha_d \Delta \boldsymbol{t} \text{ and } \boldsymbol{Z} \Leftarrow \boldsymbol{Z} + \alpha_d \Delta \boldsymbol{Z}.$$

11: **until** the real duality gap satisfies: $\mathrm{Tr}(\boldsymbol{W}\boldsymbol{Z}) - y/L \leq \epsilon$.

Output: The optimal solution $(\boldsymbol{W}^\star, y^\star, \boldsymbol{t}^\star, \boldsymbol{Z}^\star)$.

Once the optimal solution $\boldsymbol{W}^\star$ is determined, we can define

$$\boldsymbol{W}^\star = \boldsymbol{W}_l^\star = \begin{bmatrix} \boldsymbol{W}_{l,l}^\star & \boldsymbol{W}_{l,L+l}^\star \\ \boldsymbol{W}_{L+l,l}^\star & \boldsymbol{W}_{L+l,L+l}^\star \end{bmatrix} \tag{35}$$

where $l = 1, 2, \cdots, L$. According (17) to (20), it can be readily concluded that

$$\boldsymbol{W}^\star = \begin{bmatrix} \boldsymbol{I}_L \otimes \boldsymbol{W}_{l,l}^\star & \boldsymbol{I}_L \otimes \boldsymbol{W}_{l,L+l}^\star \\ \boldsymbol{I}_L \otimes \boldsymbol{W}_{L+l,l}^\star & \boldsymbol{I}_L \otimes \boldsymbol{W}_{L+l,L+l}^\star \end{bmatrix} \tag{36}$$

which can further determine $\boldsymbol{X}^\star$ via Proposition 2.

Up to now, we have successfully solved the large-scale quasi-convex optimization problem (15) and further approximate the problem (11). It is seen that both the block-sparse structure and SDR technique are utilized to facilitate us to tackle the nonconvex optimization problem (11). Hence, the proposed BSDR algorithm for one-bit MIMO radar waveform design is summarized in Algorithm 2.

Algorithm 2 The proposed BSDR algorithm for MIMO radar one-bit waveform design

Input: Θ_s, Θ_m, E, N and L.

1: **Initialize**: Seed the design parameter E, N and L.

2: Compute $\alpha = \sqrt{E/2NL}$.

3: Obtain the transmit steering vector $\boldsymbol{a}(\theta)$ by (6).

4: Calculate the complex matrix $\boldsymbol{A}_s$ and $\boldsymbol{A}_m$ as follows:

$$\boldsymbol{A}_s = \int_{\Theta_s} \boldsymbol{a}^*(\theta)\boldsymbol{a}^{\mathrm{T}}(\theta)\mathrm{d}\theta \text{ and } \boldsymbol{A}_m = \int_{\Theta_m} \boldsymbol{a}^*(\theta)\boldsymbol{a}^{\mathrm{T}}(\theta)\mathrm{d}\theta.$$

5: Construct the real matrix $\boldsymbol{A}_{m,r}$ and $\boldsymbol{A}_{s,r}$ through (19b).

6: Obtain the optimal solution $\boldsymbol{W}^\star$ via Algorithm 1.

7: Reconstruct $\boldsymbol{W}^\star$ from (22).

8: Compute $\boldsymbol{X}^\star = \alpha^2 \boldsymbol{W}^\star / [\boldsymbol{W}^\star]_{i,i}, \forall i \in \mathcal{I}$.

Output: The optimal solution $\boldsymbol{X}^\star$.

3.2 The One-bit Approximation Procedures

Having determined the optimal $\boldsymbol{X}^\star$, what we are interested in is how to synthesize the one-bit waveform sequence $\boldsymbol{x}_r^\star$ to allow $\boldsymbol{X}^\star = \boldsymbol{x}_r^\star \boldsymbol{x}_r^{\star\mathrm{T}}$. One simple approach is consisting of directly quantizing the principle eigenvector of $\boldsymbol{X}^\star$. However, this scheme can lead to severe distortion when $\mathrm{rank}(\boldsymbol{X}^\star) \neq 1$. To overcome this problem, we adopt an efficient approach, which called Gaussian Randomization [42], to approximate the desirable one-bit waveforms and further QPSK signal waveforms.

Let us first generate a set of random vectors $\boldsymbol{g}^{(t)} \in \mathbb{R}^{2NL}$ follows the Gaussian distribution $\mathcal{N}(0, \boldsymbol{X}^{\star})$, where $t = 1, 2, \cdots, T$ denotes the time index of randomization. Then, we consider to quantize $\boldsymbol{g}^{(t)}$ as following

$$\boldsymbol{x}_r^{(t)} = \mathcal{Q}(\boldsymbol{g}^{(t)}) \in \mathcal{X}_r,\ t = 1, 2, \cdots, T \tag{37}$$

By doing so, we can further choose the quantized vector with the minimum objective value for problem (11), i.e., the best energy focusing performance. The optimal index can be yielded as follows

$$t^{\star} = \arg \min_{t=1,\cdots,T} \frac{\boldsymbol{x}_r^{(t)\mathrm{T}} \boldsymbol{\Upsilon}_{s,r} \boldsymbol{x}_r^{(t)}}{\boldsymbol{x}_r^{(t)\mathrm{T}} \boldsymbol{\Upsilon}_{m,r} \boldsymbol{x}_r^{(t)}} \tag{38}$$

and we can select $\boldsymbol{x}_r^{(t^{\star})}$ as the approximation solution of problem (11). Hence, the desirable QPSK signal waveform sequence can be determined by

$$\boldsymbol{x}^{\star} = \boldsymbol{x}_r^{(t^{\star})}(1) + \mathrm{j}\boldsymbol{x}_r^{(t^{\star})}(2) \in \mathcal{X} \tag{39}$$

where $\boldsymbol{x}_r^{(t^{\star})}(1)$ and $\boldsymbol{x}_r^{(t^{\star})}(2)$ are composed of the first and last N entries of $\boldsymbol{x}_r^{(t^{\star})}$, respectively. Noticed that the empirical choice $T = 100 - 150$ is sufficient to achieve a good approximation performance. The one-bit approximation with Gaussian randomization procedures can be summarized in Algorithm 3.

Algorithm 3 One-bit approximation with Gaussian randomization procedures

Input: $\boldsymbol{X}^{\star}$, Θ_s and Θ_m.

1: **Initialize**: Seed the maximum randomization times T and the counter: $t \leftarrow 0$.

2: Calculate $\boldsymbol{\Upsilon}_m$ and $\boldsymbol{\Upsilon}_s$ through (9).

3: Calculate $\boldsymbol{\Upsilon}_{m,r}$ and $\boldsymbol{\Upsilon}_{s,r}$ through (12).

4: **repeat**

5: Generate a Gaussian random vector $\boldsymbol{g}^{(t)} \sim \mathcal{N}(0, \boldsymbol{X}^{\star})$.

6: Quantize the generated vector as $\boldsymbol{x}_r^{(t)} = \mathcal{Q}(\boldsymbol{g}^{(t)})$.

7: Compute the objective value of problem (11):

$$\frac{\boldsymbol{x}_r^{(t)\mathrm{T}} \boldsymbol{\Upsilon}_{s,r} \boldsymbol{x}_r^{(t)}}{\boldsymbol{x}_r^{(t)\mathrm{T}} \boldsymbol{\Upsilon}_{m,r} \boldsymbol{x}_r^{(t)}}.$$

8: Counter increase: $t \leftarrow t+1$.

9: **until** the counter t reaches to T.

10: Select the counter $t^{\star}$ corresponding to smallest objective value.

11: Choose $\boldsymbol{x}_r^{(t^{\star})}$ as the designed one-bit waveform sequence.

12: Recover $\boldsymbol{x}^{\star}$ via (39) as the desired QPSK signals.

Output: $\boldsymbol{x}^{\star}$

4 Complexity and Performance Analysis

In this section, we dedicate to analyzing the computational costs of the proposed BSDR method in terms of required number of real-value multiplications. For comparison, the complexity of exhaustive search scheme and ADMM are also studied in the sequel (Tab.1).

Tab. 1 Computational complexity for existing algorithm

Method	Required real-value multiplications
Exhaustive search	$4^{NL+1}N^2L^2$
ADMM	$F\left(4N^2L^2 + 5NL\right)$
BSDR	$(2N)^{3.5} + 4TN^2L^2$

4.1 Complexity of Exhaustive Search

Described as the problem (11), the one-bit signal waveform sequence ($\boldsymbol{x}_r \in \mathcal{X}_r$) should be properly synthesised such that the corresponding ISMR is minimized. To deal with this problem, the exhaustive search method should first calculate all the possible signal combinations. Then it should select the best one under the optimal criterion. As for each binary sequence $\boldsymbol{x}_r \in \mathcal{X}_r^{2NL}$, there are 4^{NL} different combinations. Furthermore, for each combination, it takes $4N^2L^2$ real-value multiplications to calculate the objective function of problem (11). Therefore, the total number of required real-valued multiplications for exhaustive search scheme can be expressed as

$$\boldsymbol{C}_{\mathrm{ES}} = 4^{NL+1}N^2L^2 \tag{40}$$

It is concluded from (40) that the exhaustive search scheme is impractical in the large-scale

data regime due to the enormously computational burden.

4.2 Complexity of ADMM Method

Let us discuss the complexity of one-bit waveform design by using ADMM framework. As illustrated in [29], the constant modulus (CM) signal waveform can be properly designed for MIMO radar with ∞-bit DACs. In order to adapt the synthesized CM waveform to one-bit MIMO system, one straightforward approach is to directly quantized it into the one-bit counterpart. It is noted that the complexity of this kind of algorithm is linear with the number of iteration. In each iteration, it takes $4N^2L^2$ real multiplications to compute the derivation of quadratic fractional function and $5NL$ real multiplications for the remaining five variables. Consequently, the total number of required real-valued multiplications for CM waveform design via ADMM can be given by

$$\boldsymbol{C}_{\text{ADMM}} = F(4N^2L^2 + 5NL) \tag{41}$$

where F denotes the required maximum iteration time. It is seen from (41) the complexity of ADMM based scheme is also considerable especially when the large number of iteration is used to pursuit better performance.

4.3 Complexity of Proposed BSDR Method

In the following, we focus on evaluating the complexity of the proposed BSDR algorithm. Firstly, our method is consider to solve the semidefinite programming (SDP) problem (20) with worst-case $(2N)^{3.5}$ real multiplications. Next, we use the Gaussian Randomization method to approximate the desired one-bit waveform which takes $4TN^2L^2$ real multiplications. Hence, the total number of required real-valued multiplications for the proposed BSDR method can be expressed as follows

$$\boldsymbol{C}_{\text{BSDR}} = (2N)^{3.5} + 4TN^2L^2 \tag{42}$$

Based on the above analysis, it is observed that the required complexity of our proposed BSDR method is comparable to ADMM based algorithm when the number of transmit antenna N is moderate but the discrete time sample is large (generally greater than 100). It is mainly because that our method has successfully modified the $2NL \times 2NL$ dimension SDP problem (16) to $2N \times 2N$ counterpart, i.e., SDP (31). To verify our analysis, the computational time of each method will be demonstrated in the next section.

4.4 Performance of Proposed BSDR Method

We continue to study the performance of our proposed algorithm. Clarified by the previous section, we can see the difference between the problem (11) and (20) is that the latter drops the rank-1 constraint and just synthesizes the covariance of transmitted signal waveform. Therefore, we have to factorize the optimal covariance matrix as $\boldsymbol{X}^\star = \boldsymbol{x}_r^\star \boldsymbol{x}_r^{\star\text{T}}$. In fact, this procedure is a nonconvex optimization problem and hard to tackle. This prompt us find an approximation solution of the rank-1 factorization problem through randomization method with a moderate complexity. That is why the performance of our proposed waveform design algorithm is largely depend on the accuracy of approximation. Fortunately, as [26], the random approximation can achieve excellent performance even though a moderate amount of iterations.

5 Simulation Results

In this section, some numerical simulations are presented to demonstrate the performance of BSDR-based method for MIMO radar transmit waveform synthesis with one-bit DACs. The transmitter deploys an uniform linear array with half-wavelength spacing between adjacent antennas. Without loss the generality, the total transmit power is set to $E = 1$. The whole spatial domain, i.e., Θ =[–90°, 90°], is uniformly sampled with 1° step-size.

5.1 Transmit Waveform Design with Single Mainlobe

Firstly, let us consider one mainlobe situation. The mainlobe is ranged from [–10°, 10°]. Fig. 1

expresses the objective value in (20) versus the number of iteration for our specialized IPA in one mainlobes setting by considering $L = 100$ and different numbers of antenna elements. It is observed that the objective value in our method is monotonically decrease as the increasing of iteration number in different transmit element scenario. Hence, the proposed IPA achieves good convergence performance. Fig. 2 presents 2D visualization of the designed beampattern versus discrete samples number for our method. We can easily see that the majority of transmit energy can be concentrated into the mainlobe regions for different discrete samples number. This exhibits the robustness of the proposed method.

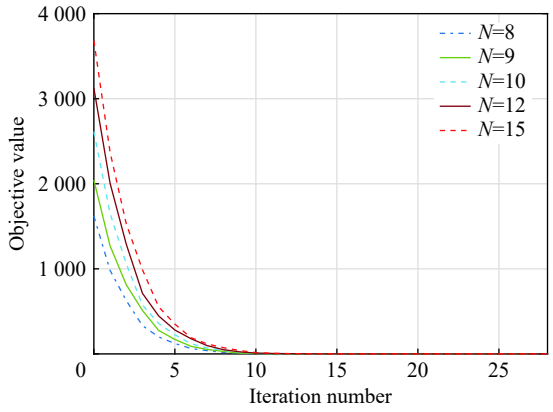

Fig. 1 The objective functions in (20) versus the iteration number, $L = 100$, one mainlobe

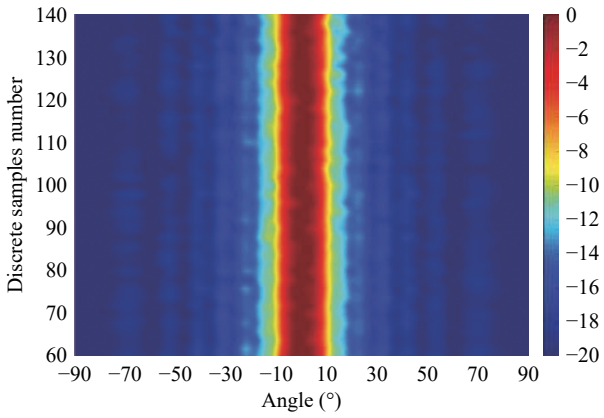

Fig. 2 Illustration of the synthesized transmit beampatterns, one mainlobe

5.2 Transmit Waveform Design with Two Mainlobes

In this subsection, let us consider two mainlobes situation. The mainlobes are ranged from $[-40°, -23°] \cup [23°, 40°]$. Fig. 3 shows the objective value in (20) versus the number of iteration for our specialized IPA in two mainlobes setting by considering $L = 100$ and different numbers of antenna elements. Again, it is seen that the proposed IPA has preferable convergence property.

Fig. 4 presents 2D visualization of the designed beampattern versus discrete samples number. Even in different discrete samples, our method can provide a stable energy gain within predefined mainlobes and express good sidelobe suppression.

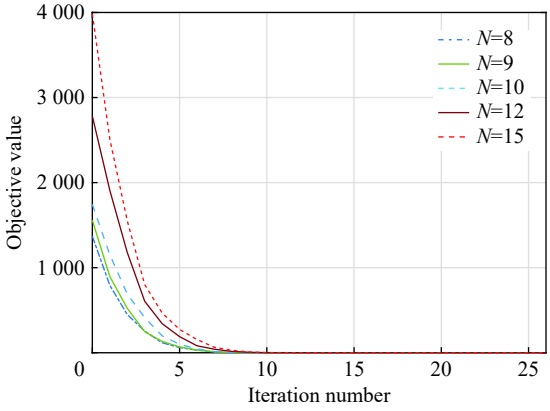

Fig. 3 The objective functions in (20) versus the iteration number, $L = 100$, two mainlobes

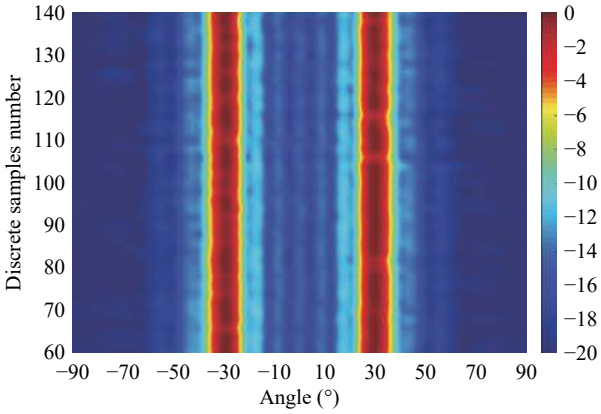

Fig. 4 Illustration of the synthesized transmit beampatterns, two mainlobes

Fig. 5 expresses the synthesized beampatterns for different methods with $N = 15$ transmitters. Traditional MIMO radar provides an uniform transmit power distribution due to the emitting of orthogonal waveform. It is easily ob-

served that the best sidelobe performance is achieved by the ADMM algorithm with ∞-bit DACs [29]. This is mainly caused that ∞-bit DACs have extended degree of freedoms for the transmit space-time waveform. Meanwhile, our designed pattern has lower sidelobe level compared with ∞-bit ADMM (directly quantize [29] into one-bit setting).

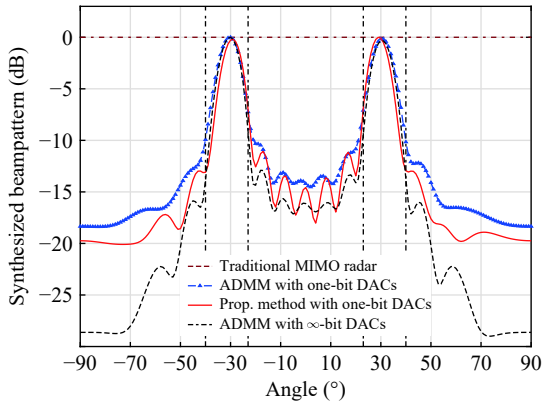

Fig. 5 Comparison of the designed transmit beampattern with different method, $L = 100$, two mainlobes

5.3 Transmit Waveform Design with Three Mainlobes

Finally, we consider that there are three mainlobes which arranged in $[-50°, -30°] \cup [-6°, 6°] \cup [30°, 50°]$. Fig. 6 shows the objective value in (20) versus the number of iteration for our specialized IPA in three mainlobes setting. The initial value becomes large as the increasing of transmit element. But all of them can converge to a tiny value. Fig. 7 also provide 2D visualization of the designed beampattern versus discrete samples number. It is seen that a large number of transmit energy can be focused as expected even in three mainloses situation. Fig. 8 expresses the synthesized beampatterns for different methods with $N = 15$ transmitters. If three mainloes are considered, ADMM method can not provide a planned results especially in the middle sector. However, our method still has a stable energy focusing performance at the interested angles. At the same time, the sidelobe of the proposed BSDR method is well controlled in a favorable level.

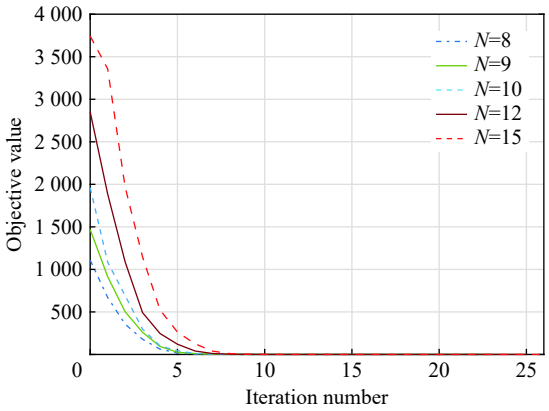

Fig. 6 The objective functions in (20) versus the iteration number, $L = 100$, three mainlobes

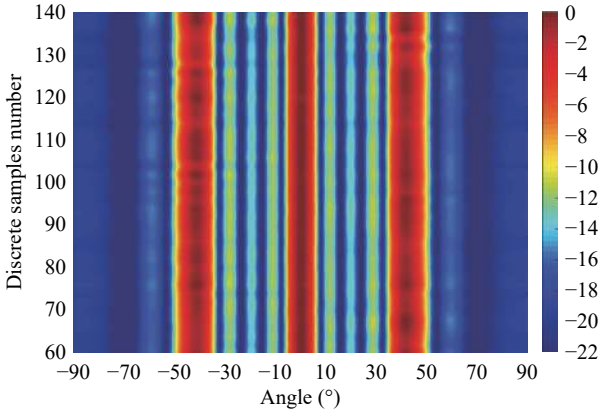

Fig. 7 Illustration of the synthesized transmit beampatterns, three mainlobes

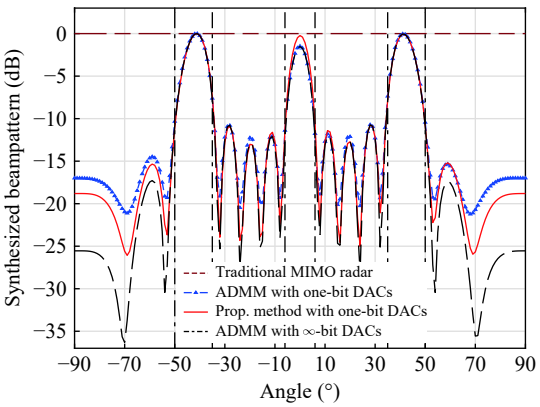

Fig. 8 Comparison of the designed transmit beampattern with different method, $L = 100$, three mainlobes

6 Conclusion

In this paper, a new transmit waveform design algorithm for MIMO radar equipped with one-bit DACs is proposed. To solve the resulting optimization problem which involves a quadratic frac-

tional objective and discrete constraint, the SDR technique is first used to reformulate the CFQP into its convex counterpart. Then, the scale of SDP problem is greatly reduced by leveraging on the specific block-sparse structure of the integral matrix. Meanwhile, a specialized primal-dual IPA is devised to deal with the reduced problem. Lastly, the Gaussian randomization method is utilized to approximate a desirable one-bit transmit waveform sequence. Compared with ∞-bit DACs, the degree of freedom (DOF) of our design is reduced due to binary constraint. However, in the one-bit DACs scenario, the transmit beampattern of our proposed algorithm can express the following preferable features: (i) the amount of transmit energy can be focused into the mainlobe region as much as possible; (ii) the leakage energy which radiates to the sidelobe region is minimized. Simulation results demonstrate that our proposed method achieves the better performance compared to the state-of-the-art one.

Appendix A Proof of Lemma 1

Substitute (9) into (12), it is derived that $\boldsymbol{\Upsilon}_{s,r}$ has the following expression

$$\boldsymbol{\Upsilon}_{s,r}=\begin{bmatrix}\boldsymbol{I}_L\otimes\mathrm{Re}\{\boldsymbol{A}_s\} & -\boldsymbol{I}_L\otimes\mathrm{Im}\{\boldsymbol{A}_s\}\\ \boldsymbol{I}_L\otimes\mathrm{Im}\{\boldsymbol{A}_s\} & \boldsymbol{I}_L\otimes\mathrm{Re}\{\boldsymbol{A}_s\}\end{bmatrix} \tag{43}$$

It is observed that $\boldsymbol{\Upsilon}_{s,r}$ is composed by four sparse block matrices. Meanwhile, according to (17), we find that $\boldsymbol{W}$ can be also seen with four parts which are divided through the dot line. For simplicity, let us rewrite $\boldsymbol{W}$ as follows

$$\boldsymbol{W}=\begin{bmatrix}\boldsymbol{W}_{b,1} & \boldsymbol{W}_{b,2}\\ \boldsymbol{W}_{b,3} & \boldsymbol{W}_{b,4}\end{bmatrix} \tag{44}$$

where $\boldsymbol{W}_{b,i}, i=1,\cdots,4$ is corresponding to these four block matrices, respectively. Hence, we have

$$\begin{aligned}\mathrm{Tr}(\boldsymbol{\Upsilon}_{s,r}\boldsymbol{W})=&\mathrm{Tr}\left((\boldsymbol{I}_L\otimes\mathrm{Re}\{\boldsymbol{A}_s\})(\boldsymbol{W}_{b,1}+\boldsymbol{W}_{b,4})\right)+\\ &\mathrm{Tr}\left((\boldsymbol{I}_L\otimes\mathrm{Im}\{\boldsymbol{A}_s\})(\boldsymbol{W}_{b,2}-\boldsymbol{W}_{b,3})\right)\end{aligned} \tag{45}$$

Replacing the $\boldsymbol{W}_{b,i}, i=1,\cdots,4$ by its corresponding matrices in (17), it is seen that the right side of equation (45) can be further expanded as

$$\begin{aligned}\mathrm{Tr}(\boldsymbol{\Upsilon}_{s,r}\boldsymbol{W})=&\sum_{l=1}^{L}\mathrm{Tr}\left(\mathrm{Re}\{\boldsymbol{A}_s\}\boldsymbol{W}_{l,l}\right)-\\ &\sum_{l=1}^{L}\mathrm{Tr}\left(\mathrm{Im}\{\boldsymbol{A}_s\}\boldsymbol{W}_{L+l,l}\right)+\sum_{l=1}^{L}\mathrm{Tr}\left(\mathrm{Im}\{\boldsymbol{A}_s\}\boldsymbol{W}_{l,L+l}\right)+\\ &\sum_{l=1}^{L}\mathrm{Tr}\left(\mathrm{Re}\{\boldsymbol{A}_s\}\boldsymbol{W}_{L+l,L+l}\right)\end{aligned} \tag{46}$$

By doing so, one can immediately obtained

$$\mathrm{Tr}(\boldsymbol{\Upsilon}_{s,r}\boldsymbol{W})=\sum_{l=1}^{L}\mathrm{Tr}\left(\begin{bmatrix}\mathrm{Re}\{\boldsymbol{A}_s\} & -\mathrm{Im}\{\boldsymbol{A}_s\}\\ \mathrm{Im}\{\boldsymbol{A}_s\} & \mathrm{Re}\{\boldsymbol{A}_s\}\end{bmatrix}\mathrm{W}_l\right) \tag{47}$$

Substituting (19b) into (47), we have

$$\mathrm{Tr}(\boldsymbol{\Upsilon}_{s,r}\boldsymbol{W})=\sum_{l=1}^{L}\mathrm{Tr}\left(\boldsymbol{A}_{s,r}\boldsymbol{W}_l\right) \tag{48}$$

Similar to above discussions, it is easily derived

$$\mathrm{Tr}(\boldsymbol{\Upsilon}_{m,r}\boldsymbol{W})=\sum_{l=1}^{L}\mathrm{Tr}\left(\boldsymbol{A}_{m,r}\boldsymbol{W}_l\right)=1 \tag{49}$$

The proof is completed.

References:

[1] J. Li and P. Stoica,"MIMO radar with colocated antennas," *IEEE Signal Processing Magazine*, vol. 24, no. 5, pp. 106-114, 2007.

[2] A. M. Haimovich, R. S. Blum, and L. J. Cimini,"MIMO radar with widely separated antennas," *IEEE Signal Processing Magazine*, vol. 25, no. 1, pp. 116-129, 2008.

[3] I. Bekkerman and J. Tabrikian,"Target detection and localization using MIMO radars and sonars," *IEEE Transactions on Signal Processing*, vol. 54, no. 10, pp. 3873-3883, 2006.

[4] M. A. Jensen and J. W. Wallace,"A review of antennas and propagation for MIMO wireless communications," *IEEE Transactions on Antennas and Propagation*, vol. 52, no. 11, pp. 2810-2824, 2004.

[5] H. Godrich, A. M. Haimovich, and R. S. Blum,"Target localization accuracy gain in MIMO radar-based systems," *IEEE Transactions on Information Theory*, vol. 56, no. 6, pp. 2783-2803, 2010.

[6] N. H. Lehmann, A. M. Haimovich, R. S. Blum, and L. Cimini, "High resolution capabilities of MIMO radar, " in *2006 Fortieth Asilomar Conference on*

Signals, Systems and Computers, Oct 2006, pp. 25–30.

[7] Q. He, N. H. Lehmann, R. S. Blum, and A. M. Haimovich,"MIMO radar moving target detection in homogeneous clutter," *IEEE Transactions on Aerospace and Electronic Systems*, vol. 46, no. 3, pp. 1290-1301, 2010.

[8] P. Stoica, J. Li, and Y. Xie,"On probing signal design for MIMO radar," *IEEE Transactions on Signal Processing*, vol. 55, no. 8, pp. 4151-4161, 2007.

[9] D. R. Fuhrmann and G. S. Antonio,"Transmit beamforming for MIMO radar systems using signal cross-correlation," *IEEE Transactions on Aerospace and Electronic Systems*, vol. 44, no. 1, pp. 171-186, 2008.

[10] P. Stoica, J. Li, and X. Zhu,"Waveform synthesis for diversity-based transmit beampattern design," *IEEE Transactions on Signal Processing*, vol. 56, no. 6, pp. 2593-2598, 2008.

[11] S. Ahmed, J. S. Thompson, Y. R. Petillot, and B. Mulgrew,"Unconstrained synthesis of covariance matrix for MIMO radar transmit beampattern," *IEEE Transactions on Signal Processing*, vol. 59, no. 8, pp. 3837-3849, 2011.

[12] S. Ahmed and M. Alouini,"MIMO radar transmit beampattern design without synthesising the covariance matrix," *IEEE Transactions on Signal Processing*, vol. 62, no. 9, pp. 2278-2289, 2014.

[13] G. Hua and S. S. Abeysekera,"MIMO radar transmit beampattern design with ripple and transition band control," *IEEE Transactions on Signal Processing*, vol. 61, no. 11, pp. 2963-2974, 2013.

[14] Z. Cheng, Y. Zhao, H. Li, and P. Shui,"Sparse representation framework for MIMO radar transmit beampattern matching design," *IEEE Transactions on Aerospace and Electronic Systems*, vol. 53, no. 1, pp. 520-529, 2017.

[15] Z. Cheng, Z. He, S. Zhang, and J. Li,"Constant modulus waveform design for MIMO radar transmit beampattern," *IEEE Transactions on Signal Processing*, vol. 65, no. 18, pp. 4912-4923, 2017.

[16] S. Ahmed, J. S. Thompson, Y. R. Petillot, and B. Mulgrew,"Finite alphabet constant-envelope waveform design for MIMO radar," *IEEE Transactions on Signal Processing*, vol. 59, no. 11, pp. 5326-5337, 2011.

[17] K. Alhujaili, V. Monga, and M. Rangaswamy,"Transmit MIMO radar beampattern design via optimization on the complex circle manifold," *IEEE Transactions on Signal Processing*, vol. 67, no. 13, pp. 3561-3575, 2019.

[18] B. Tang and J. Tang,"Joint design of transmit waveforms and receive filters for MIMO radar space-time adaptive processing," *IEEE Transactions on Signal Processing*, vol. 64, no. 18, pp. 4707-4722, 2016.

[19] G. Cui, X. Yu, V. Carotenuto, and L. Kong,"Space-time transmit code and receive filter design for colocated MIMO radar," *IEEE Transactions on Signal Processing*, vol. 65, no. 5, pp. 1116-1129, 2017.

[20] S. Imani and S. A. Ghorashi,"Transmit signal and receive filter design in colocated MIMO radar using a transmit weighting matrix," *IEEE Signal Processing Letters*, vol. 22, no. 10, pp. 1521-1524, 2015.

[21] W. Zhu and J. Tang,"Robust design of transmit waveform and receive filter for colocated MIMO radar," *IEEE Signal Processing Letters*, vol. 22, no. 11, pp. 2112-2116, 2015.

[22] L. Wu, P. Babu, and D. P. Palomar,"Transmit waveform/receive filter design for MIMO radar with multiple waveform constraints," *IEEE Transactions on Signal Processing*, vol. 66, no. 6, pp. 1526-1540, 2018.

[23] M. Shaghaghi, R. S. Adve, and G. Shehata,"Training-based adaptive transmit receive beamforming for MIMO radars," *IEEE Transactions on Aerospace and Electronic Systems*, vol. 53, no. 6, pp. 2899-2912, 2017.

[24] Z. Cheng, B. Liao, Z. He, J. Li, and J. Xie,"Joint design of the transmit and receive beamforming in MIMO radar systems," *IEEE Transactions on Vehicular Technology*, vol. 68, no. 8, pp. 7919-7930, 2019.

[25] A. Hassanien and S. A. Vorobyov,"Transmit energy focusing for DOA estimation in MIMO radar with colocated antennas," *IEEE Transactions on Signal Processing*, vol. 59, no. 6, pp. 2669-2682, 2011.

[26] H. Xu, R. S. Blum, J. Wang, and J. Yuan,"Colocated MIMO radar waveform design for transmit beampattern formation," *IEEE Transactions on Aerospace and Electronic Systems*, vol. 51, no. 2, pp. 1558-1568, 2015.

[27] A. Aubry, A. D. Maio, and Y. Huang,"MIMO radar beampattern design via PSL/ISL optimiza-

tion," *IEEE Transactions on Signal Processing*, vol. 64, no. 15, pp. 3955-3967, 2016.

[28] W. Fan, J. Liang, and J. Li,"Constant modulus MIMO radar waveform design with minimum peak sidelobe transmit beampattern," *IEEE Transactions on Signal Processing*, vol. 66, no. 16, pp. 4207-4222, 2018.

[29] Z. Cheng, C. Han, B. Liao, Z. He, and J. Li,"Communication-aware waveform design for MIMO radar with good transmit beampattern," *IEEE Transactions on Signal Processing*, vol. 66, no. 21, pp. 5549-5562, 2018.

[30] M. Grant and S. Boyd, "CVX: Matlab software for disciplined convex programming, version 2.1, " http://cvxr.com/cvx, 2016.

[31] Z. Cheng, B. Liao, Z. He, J. Li, and J. Xie, "Transmit beampattern design for mimo radar with one-bit DACs, " in *ICASSP 2019 - 2019 IEEE International Conference on Acoustics, Speech and Signal Processing (ICASSP)*, 2019, pp. 4275–4279.

[32] Z. Cheng, B. Liao, Z. He, and J. Li,"Transmit signal design for large-scale MIMO system with 1-bit DACs," *IEEE Transactions on Wireless Communications*, vol. 18, no. 9, pp. 4466-4478, 2019.

[33] S. Jacobsson, G. Durisi, M. Coldrey, T. Goldstein, and C. Studer,"Quantized precoding for massive MU-MIMO," *IEEE Transactions on Communications*, vol. 65, no. 11, pp. 4670-4684, 2017.

[34] A. Li, C. Masouros, F. Liu, and A. L. Swindlehurst,"Massive MIMO 1-bit DAC transmission: A low-complexity symbol scaling approach," *IEEE Transactions on Wireless Communications*, vol. 17, no. 11, pp. 7559-7575, 2018.

[35] L. Chu, F. Wen, L. Li, and R. Qiu,"Efficient nonlinear precoding for massive MIMO downlink systems with 1-bit DACs," *IEEE Transactions on Wireless Communications*, vol. 18, no. 9, pp. 4213-4224, 2019.

[36] S. Jacobsson, G. Durisi, M. Coldrey, and C. Studer,"Linear precoding with low-resolution DACs for massive mu-mimo-ofdm downlink," *IEEE Transactions on Wireless Communications*, vol. 18, no. 3, pp. 1595-1609, 2019.

[37] M. Deng, Z. Cheng, X. Lu, and Z. He,"Binary waveform design for MIMO radar with good transmit beampattern performance," *Electronics Letters*, vol. 55, no. 19, pp. 1061-1063, 2019.

[38] Z. Cheng, S. Shi, Z. He, and B. Liao,"Transmit sequence design for dual-function radar-communication system with one-bit DACs," *IEEE Transactions on Wireless Communications*, vol. 20, no. 9, pp. 5846-5860, 2021.

[39] T. Wei, P. Chu, Z. Cheng, and B. Liao, "Transmit beampattern design for mimo radar with one-bit dacs via block-sparse SDR, " in *2020 IEEE 11th Sensor Array and Multichannel Signal Processing Workshop (SAM)*, 2020, pp. 1–5.

[40] S. Boyd and L. Vandenberghe, *Convex optimization*. New York: Cambridge University Press, 2008.

[41] P. Amaral, I. Bomze, and J. Judice,"Copositivity and constrained fractional quadratic problems," *Mathematical Programming*, vol. 146, no. 1-2, pp. 325-350, 2014.

[42] Z. Luo, W. Ma, A. M. So, Y. Ye, and S. Zhang,"Semidefinite relaxation of quadratic optimization problems," *IEEE Signal Processing Magazine*, vol. 27, no. 3, pp. 20-34, 2010.

[43] T. Chang, C. Hsin, W. Ma, and C. Chi,"A linear fractional semidefinite relaxation approach to maximum-likelihood detection of higher-order QAM OSTBC in unknown channels," *IEEE Transactions on Signal Processing*, vol. 58, no. 4, pp. 2315-2326, 2010.

[44] A. De Maio, Y. Huang, D. P. Palomar, S. Zhang, and A. Farina,"Fractional QCQP with applications in ML steering direction estimation for radar detection," *IEEE Transactions on Signal Processing*, vol. 59, no. 1, pp. 172-185, 2011.

[45] J. F. Sturm,"Using SeDuMi 1.02, a Matlab toolbox for optimization over symmetric cones," *Optimization Methods and Software*, vol. 11, pp. 625-653, 1999.

[46] C. Helmberg, F. Rendl, R. J. Vanderbei, and H. Wolkowicz,"An interior-point method for semidefinite programming," *SIAM Journal on Optimization*, vol. 6, pp. 342-361, 1996.

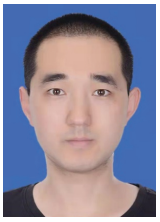

Tong Wei received the B.Eng. degree from Hainan University in 2017 and M. Eng degree from Shenzhen University in 2020. He is currently pursuing the Ph.D. degree in electrical and electronic engineering at University of Luxembourg, Luxembourg. His main research interests are radar signal processing, convex optimization and its applications.

Bin Liao received the B.Eng. and M.Eng degrees from Xidian University, Xi'an, China, in 2006 and 2009, respectively, and received his Ph.D. degree from The University of Hong Kong, Hong Kong, in 2013. From September 2013 to January 2014, he was a Research Assistant with the Department of Electrical and Electronic Engineering, The University of Hong Kong, Hong Kong. From August 2016 to October 2016, he was a Research Scientist with the Department of Electrical and Electronic Engineering, The University of Hong Kong, Hong Kong. He is currently an Associate Professor in the College of Information Engineering, Shenzhen University, Shenzhen, China. He is a recipient of the Best Paper Award at the 21st International Conference on Digital Signal Processing (2016 DSP) and 22nd International Conference on Digital Signal Processing (2017 DSP). His research interests include sensor array processing, adaptive filtering, convex optimization, with applications to radar, navigation and communications.

Dr. Liao is currently a member of the Sensor Array and Multichannel (SAM) Technical Committee of the IEEE Signal Processing Society. He was an Associate Editor of IEEE ACCESS from 2017 to 2019. He is currently an Associate Editor of IEEE Transactions on Aerospace and Electronic Systems, IET Signal Processing, and Multidimensional Systems and Signal Processing.